Available online at www.sciencedirect.com
ScienceDirect
Biosensors and Bioelectronics 23 (2008) 1666–1673
BIOSENSORS & BIOELECTRONICS
www.elsevier.com/locate/bios

Horseradish peroxidase-functionalized gold nanoparticle label for amplified immunoanalysis based on gold nanoparticles/carbon nanotubes hybrids modified biosensor

Rongjing Cui, Haiping Huang, Zhengzhi Yin, Di Gao, Jun-Jie Zhu *

Key Laboratory of Analytical Chemistry for Life Science (MOE), School of Chemistry and Chemical Engineering, Nanjing University, Nanjing 210093, People's Republic of China

Received 18 October 2007; received in revised form 2 January 2008; accepted 29 January 2008
Available online 13 February 2008

Abstract

This paper describes the combination of electrochemical immunosensor using gold nanoparticles (GNPs)/carbon nanotubes (CNTs) hybrids platform with horseradish peroxidase (HRP)-functionalized gold nanoparticle label for the sensitive detection of human IgG (HIgG) as a model protein. The GNPs/CNTs nanohybrids covered on the glass carbon electrode (GCE) constructed an effective antibody immobilization matrix and made the immobilized biomolecules hold high stability and bioactivity. Enhanced sensitivity was obtained by using bioconjugates featuring HRP labels and secondary antibodies (Ab_2) linked to GNPs at high HRP/Ab_2 molar ratio. The approach provided a linear response range between 0.125 and 80 ng/mL with a detection limit of 40 pg/mL. The immunosensor showed good precision, acceptable stability and reproducibility and could be used for the detection of HIgG in real samples, which provided a potential alternative tool for the detection of protein in clinical laboratory.

Keywords: Electrochemical biosensor; Amplified immunoassay; Hybrids

1. Introduction

Achieving high sensitivity is a major goal in immunoassay, such as the monitoring of disease markers and infectious agents or biothreat agents. The achievement of high sensitivity requires innovative approaches that couple different amplification platforms and amplification processes (Wang, 2005). By incorporation with nanoparticles (NPs), the enormous signal enhancement associated with the use of NPs amplifying labels and with the formation of NPs/biomolecule conjugations provides the basis for ultrasensitive electrical detection of trace biomolecule (Cui et al., 2007; Daniel and Astruc, 2004; Katz and Willner, 2004). It has been reported that the NPs-based amplification platforms and amplification processes dramatically enhanced the intensity of the electrochemical signal and lead to ultrasensitive bioassays (Hansen et al., 2006; Das et al., 2006; Yu et al., 2006). For example, Wang et al. have developed a highly sensitive bioelectronic protocol for detecting proteins based on CNTs as carriers for numerous enzyme tags (Wang et al., 2003). Further sensitivity enhancement was achieved by a layer-by-layer (LbL) assembly of multilayer enzymes films on the CNTs template (Munge et al., 2005). The coupling of CNTs carriers and protein multilayer architectures were shown to maximize the ratio of enzyme tags per binding event and hence to offer a remarkably high amplification factor. Among the various NPs, gold nanoparticles (GNPs) have been recognized as a versatile and efficient label for the conjugation of biomolecules due to their rapid and simple chemical synthesis, a narrow size distribution, and efficient coating by thiols or other bioligands (Katz et al., 2004; Merkocüi et al., 2005; Pumera et al., 2005; Zhang et al., 2002; Schneider et al., 2000a, 2000b). Recently, a novel double-codified nanolabel based on GNPs modified with horseradish peroxidase (HRP) conjugated antibody for enhanced immunoanalysis was reported (Ambrosi et al., 2007). Yet, amplified transduction of biological recognition events remains a major challenge to electrical bioassays.

Another long-standing goal in electrochemical immunosensors is stability and activity of the immobilized biocomponents on solid support. Taking account of the advantages of GNPs

* Corresponding author. Fax: +86 25 83594976.
E-mail address: jjzhu@nju.edu.cn (J.-J. Zhu).

0956-5663/$ – see front matter © 2008 Elsevier B.V. All rights reserved.
doi:10.1016/j.bios.2008.01.034

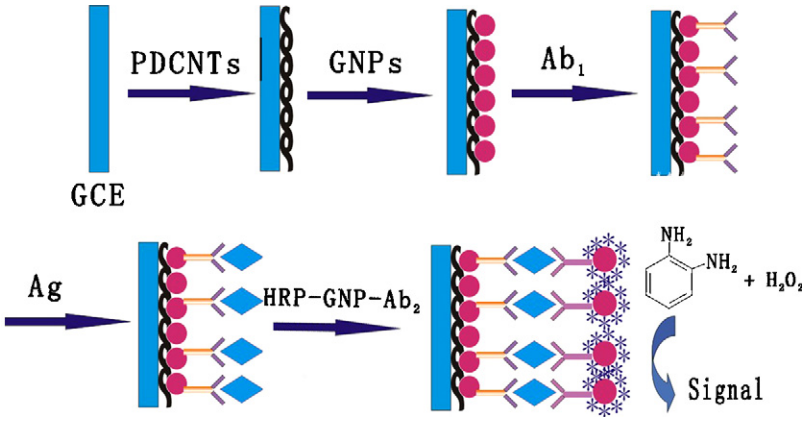

Fig. 1. The immunoassay procedure of GNPs/PDCNTs modified immunosensor using HRP–GNPs–Ab_2 conjugates as label.

and CNTs, the hybrid composite has more potential applications for the generation of electrochemical sensor. Thus, the importance of the interactions between CNTs and metal NPs has also been increasingly recognized due to their remarkable properties. Some groups have demonstrated that the CNTs could be rationally functionalized and that the metal NPs could be uniformly attached to the functionalized CNTs by virtue of the electrostatic interaction between the CNTs and polyelectrolyte (i.e., poly(diallyldimethylammonium chloride) (PDDA)) (Mamedov et al., 2002; Rouse and Lillehei, 2003). It was reported these hybrids had been used to fabricate GNPs/CNTs/GOx multilayer composite through LbL assembly for glucose biosensors (Wu et al., 2007).

In this paper, we developed a novel amperometric immunosensor based on self-assemble of GNPs/CNTs hybrids on glass carbon electrode (GCE), which constructed an effective antibody immobilization matrix and made the immobilized immunocomponents hold high stability and bioactivity. Herein, we pursued a multi-label strategy that provided the advantages of enhanced sensitivity and selectivity by virtue of the "sandwich-type" immunoassay. The amplified sensitivity was enhanced by using bioconjugates featuring horseradish peroxidase labels and secondary antibodies (Ab_2) linked to GNPs at high HRP/Ab_2 ratio to replace conventional singly labeled Ab_2 (Fig. 1). To the best of our knowledge, it is not found the report about the self-assembly GNPs/CNTs hybrids as an immunosensor based on HRP–GNPs–Ab_2 conjugations.

2. Experimental section

2.1. Chemicals and materials

Multi-walled carbon nanotubes (CNTs, CVD method, purity >95%, diameter 60–100 nm, length 5–15 μm) were purchased from Nanoport. Co. Ltd. (Shenzhen, China). Human IgG (HIgG) (Ag), goat anti-human IgG (Ab_1), monoclonal mouse anti-human IgG (Ab_2) and HRP-labeled monoclonal mouse anti-human IgG (HRP–Ab_2) were purchased from Zhengzhou Chuangsheng Biochemical Reagents (Zhengzhou, China). Horseradish peroxidase (MW = 44,000), lyophilized 99% bovine serum albumin (BSA), poly(diallyldimethylammonium chloride) (20%, w/w in water, MW = 200,000–350,000), Coomassie Blue G-250, and Tween-20 were from Sigma–Aldrich. *O*-Phenylenediamine (OPD) and H_2O_2 with analytical grade were from Shanghai Biochemical Reagent Company (China). Glycine, chloroauric acid ($HAuCl_4{\cdot}3H_2O$) and trisodium citrate were obtained from Shanghai Reagent Company (Shanghai, China). All other reagents were of analytical reagent grade and used without further purification. 0.1 M PBS of various pHs were prepared by mixing the stock solutions of NaH_2PO_4 and Na_2HPO_4, and then adjusting the pH with 0.1 M NaOH and H_3PO_4. Doubly distilled water was used throughout the experiments. The GNPs used in all experiments were prepared according to the reported method by boiling $HAuC1_4$ aqueous solution with trisodium citrate (Enustun and Turkevich, 1963). The average diameter of the prepared GNPs is about 20 nm.

2.2. Apparatus

Electrochemical immunoassay measurements were performed on a CHI 660 electrochemical analyzer (Co. CHI, USA) with a conventional three-electrode system comprised of platinum wire as the auxiliary electrode, saturated calomel electrode (SCE) as the reference and a modified GCE as the working electrode. The electrochemical impedance spectroscopy analyses were performed with an Autolab PGSTAT12 (Eco chemie, BV, The Netherlands) and controlled by GPES 4.9 and FRA 4.9 softwares with a three-electrode system in the solution of 0.10 M KNO_3 containing 2.0 mM $K_3[Fe(CN)_6]/K_4[Fe(CN)_6]$. The electrochemical impedance spectra were recorded in the frequency range 0.1–1.0 × 10^5 Hz, at the formal potential (0.20 V vs. SCE) of the redox couple and with a perturbation potential of 5 mV.

The atomic force microscopy (AFM) experiments were performed on SPA-300 HV with a SPI 3800 controller (Seiko). They were carried out using the tapping mode. All images are presented without any subsequent data processing. All chips were measured in open air. Field-emission scanning electron microscopy (FESEM, JEOL JSM-6340 F) was used for imaging

topography and morphology of the self-assembled immunosensor.

2.3. Preparation of soluble PDDA-CNTs (PDCNTs)

CNTs were chemically shortened by ultrasonic agitation in a mixture of sulfuric acid and nitric acid (3:1) for about 3 h. The resulting CNTs were separated and washed repeatedly with distilled water by centrifugation until pH was ~7. The purified CNTs were functionalized with PDDA according to the following procedures: 0.5 mg/mL CNTs were dispersed into a 0.25% PDDA aqueous solution containing 0.5 M NaCl and the resulting dispersion was sonicated for 30 min to give a homogeneous black suspension. Residual PDDA polymer was removed by high-speed centrifugation and the complex was rinsed with water for at least three times. The collected complex was redispersed in water with mild sonicating to produce a stable solution of the complex, which was sonicated for 5 min immediately before preparing the films.

2.4. Fabrication of GNPs/PDCNTs modified immunosensor

The GCE with a diameter of 3 mm was used as the substrate to grow the GNPs/PDCNTs film. Prior to preparation procedure, the GCE was successively polished to a mirror finish using 0.3 and 0.05 μm alumina slurry (Beuhler) followed by rinsing thoroughly with water. After successive sonication in 1:1 nitric acid, acetone, and doubly distilled water, the electrode was rinsed with doubly distilled water and allowed to dry at room temperature. Five microliters of 5 mg/mL PDCNTs solution was dropped on the pretreated GCE and dried in a silica gel desiccator, then immersed in the GNPs solution for 30 min. After the modified GNPs/PDCNTs/GCE was thoroughly rinsed with water, the electrode was stored at 4 °C when not in use.

2.5. Preparation of the HRP–GNPs–Ab_2 bioconjugates

GNPs were coated with Ab_2 and HRP according to a documented method (Hayat, 1989; Xu, 1997). At room temperature, 1.5 μL of 5.0 mg/mL Ab_2 and 3.0 μL of 5.0 mg/mL HRP were added in 1.0 mL of the GNPs solution containing 0.04% trisodium citrate, 0.26 mM potassium carbonate, and 0.02% sodium azide. The mixture was gently mixed for 2 h, blocked by 100 μL of 1% BSA solution for 30 min at room temperature, and centrifuged at 15,000 rpm for 20 min at 4 °C. After centrifugation, the oiled drop was washed by washing buffer and resuspended in 100 μL of 1% BSA as the assay solution.

2.6. Antibody immobilization and immunoreaction procedure

Ab_1 was immobilized onto the GNPs/PDCNTs modified GCE. Five microliters of 0.5 mg/mL Ab_1 solution (50 mM PBS, pH 7.4) was spread onto the GCE surface. The electrode was incubated at 4 °C in a moisture atmosphere to avoid evaporation of solvent. After incubation for at least 15 h, they were rinsed with PBS, 0.05% Tween (PBST) to remove physically absorbed Ab_1. The electrodes were then blocked with 2% BSA + 0.05% Tween-20 solution for 1 h at room temperature, and washed with PBST. After aspiration, Ab_1 modified electrodes incubated with 60 μL of detecting Ag samples for 50 min at 37 °C. By the binding reaction between Ab_1 and Ag, the electrodes immersed into the 60 μL of diluted HRP–Ab_2 or Ab_2–GNPs–HRP bioconjugates solution for an incubation of 50 min. Finally, the electrodes were washed thoroughly with water to remove nonspecifically bound conjugations, which could cause a background response before measurement. The way to the immobilization of Ab_1 and the immunoassay procedure were shown in Fig. 1.

2.7. Measurement procedure

The immunosensor was then placed in an electrochemical cell containing 3.0 mL pH 7.0 PBS buffer, 2.0 mM OPD and 4.0 mM H_2O_2, which was deaerated thoroughly with highly pure nitrogen for 5 min and maintained in nitrogen atmosphere at room temperature. In the presence of HRP immobilized on GCE surface, the electroactive species, 2,2′-diaminoazobenzene (Zhao et al., 1992), was firstly produced. The differential pulse voltammetric (DPV) measurements were performed from −0.3 to −0.8 V with the pulse amplitude of 50 mV and the pulse width of 50 ms.

3. Results and discussion

3.1. Preparation and characterization of the immunosensor

3.1.1. FESEM

Since CNTs are chemically inert, activating their surface is an essential prerequisite for linking functional groups for anchoring GNPs. CNTs were initially oxidized by acid treatment to introduce carboxyl groups on their tips and any defect in the side walls (Liu et al., 1998). As demonstrated by previous report (Wang et al., 2007) a cationic polyelectrolyte, PDDA, was adsorbed on the surface of the CNTs by electrostatic interaction between carboxyl groups on the CNTs surface and polyelectrolyte chains. In this paper, CNTs modified by PDDA were assembled on the activated GCE surface, and then GNPs can be electrostatic absorbed to the CNTs surface. Ab_1 was finally immobilized onto the GNPs because of the strong interaction between GNPs and mercapto or primary amine groups in biomolecules. Fig. 2A displays typical FESEM images of PDCNTs, GNPs/PDCNTs, and Ab_1/GNPs/PDCNTs assembled on the GCE surfaces, respectively. It could be found that the PDDA functionalized CNTs were well-dispersed in aqueous solution and the PDCNTs homogeneously assembled on the GCE were mostly in the form of small bundles or single tubes, as could be seen from the FESEM of PDCNTs modified GCE (image a in Fig. 2A). Making a comparison between images a and b in Fig. 2A, the distinctive difference in the topography can be observed before and after the binding of GNPs. Image b in Fig. 2A shows the FESEM of GNPs/PDCNTs layers formed after the interaction between GNPs and PDCNTs. As we could see more clearly from image c (the magnification from part of the image b), the well-dispersed GNPs decorated on the walls and ends of the nanotubes quite

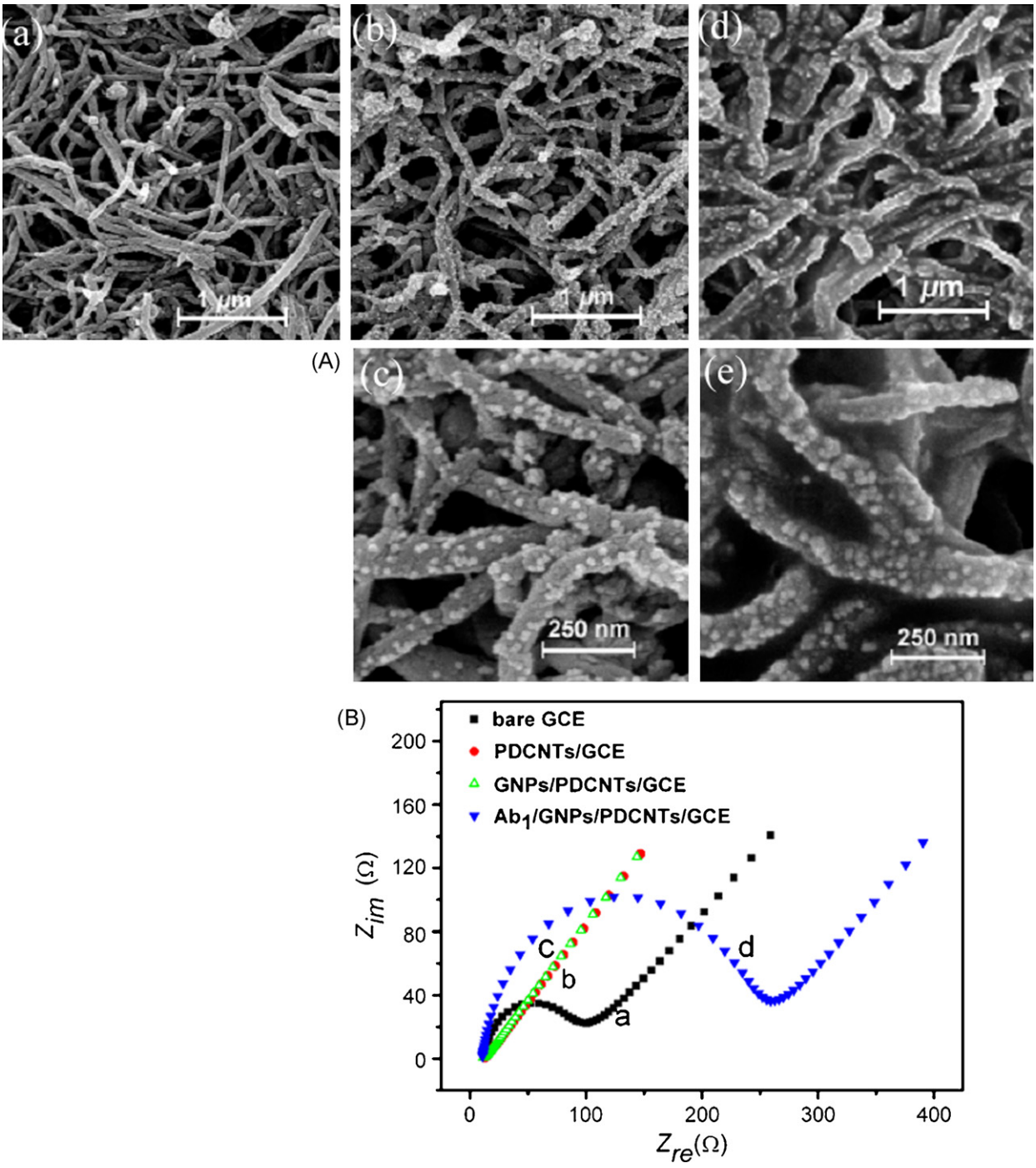

Fig. 2. (A) Representative FESEM images of PDCNTs/GCE (a), GNPs/PDCNTs/GCE (b) and its magnification (c), Ab_1/GNPs/PDCNTs/GCE (d) and its magnification (e). (B) EIS of bare GCE (a), PDCNTs/GCE (b), GNPs/PDCNTs/GCE (c), and Ab_1/GNPs/PDCNTs/GCE (d).

uniformly, and confirmed the attachment of GNPs to PDCNTs. This indicated that PDDA played a key role in the process; it acted as a bridge to connect GNPs with CNTs (Jiang et al., 2002; Wang et al., 2007). The prepared GNPs/PDCNTs modified electrodes were found to be very stable, which was illustrated by the redox process of $[Fe(CN)_6]^{3-/4-}$ in solution phase: the redox peak currents were essentially unchanged after continuously cycling the electrode for 100 cycles or after the electrodes were stored in distilled water for 1 week. Images d and e in Fig. 2 shows the Ab_1/GNPs/PDCNTs/GCE with different magnifications. Compared with images d and b in Fig. 2, it was obvious that after Ab_1 attached to the GNPs/PDCNTs modified GCE, the GNPs/PDCNTs became "fat". Moreover, it could be seen that the surface was much rougher, and richer in texture, than the surface of the GNPs/PDCNTs hybrids. We might conclude that the Ab_1 molecules were adsorbed on the surface of the GNPs/PDCNTs, where the structure of compositions was completely changed.

3.1.2. EIS

Impedance spectroscopy was reported as an effective method to monitor the feature of surface allowing the understanding of chemical transformation and processes associated with the conductive electrode surface (Bard and Faulkner, 1980). The impedance spectra include a semicircle portion and a linear portion, the semicircle portion at higher frequencies corresponds to the electron-transfer limited process, and the linear part at lower frequencies corresponds to the diffusion process. The semicircle diameter corresponds to the electron-transfer resistance (R_{et}). Fig. 2B shows the Nyquist plots of EIS for the bare GCE, PDCNTs/GCE, GNPs/PDCNTs/GCE, and Ab_1/GNPs/PDCNTs/GCE. At a bare GCE, the redox process of the $[Fe(CN)_6]^{3-/4-}$ probe showed an electron-transfer resistance of about 91 Ω (curve a in Fig. 2B). The PDCNTs and GNPs/PDCNTs modified GCE both showed a much lower resistance for the redox probe (curves b, c in Fig. 2B), implying that the PDCNTs and GNPs were both an excellent electric conducting material and accelerated the electron transfer. When Ab_1 molecules were assembled on the GNPs/PDCNTs/GCE, the electron-transfer resistance increased (curve d in Fig. 2B), suggesting that Ab_1 molecules were immobilized on the electrode and blocked the electron exchange between the redox probe and the electrode. The results were consistent with the observation from FESEM images as shown in Fig. 2A.

3.2. The immunosensor using Ab_2–GNPs–HRP bioconjugates

3.2.1. Cyclic voltammetric behavior of the immunosensor

It was well known that HRP can catalyze the oxidation reaction of OPD by H_2O_2, and the mechanism of enzymatic catalysis and oxidation was investigated previously (Porstmann and Porstmann, 1988). Fig. 3A and B shows the cyclic voltammograms of bare GCE, GNPs/PDCNTs/GCE and HRP–GNPs–Ab–Ag complexes covered GNPs/PDCNTs/GCE in different solutions. No amperometric response was observed at both bare GCE, GNPs/PDCNTs/GCE and HRP–GNPs–Ab–Ag complexes covered GNPs/PDCNTs/GCE in 0.1 M pH 7.0 PBS (curves a, b in Fig. 3A and curve a in Fig. 3B). The pretreatment GCE showed a relatively lower charging current due to the active surface of GCE. Obviously, the presence of GNPs/PDCNTs hybrids improved the electron transfer, compared with curves a and b in Fig. 3A. When 2.0 mM OPD was added to

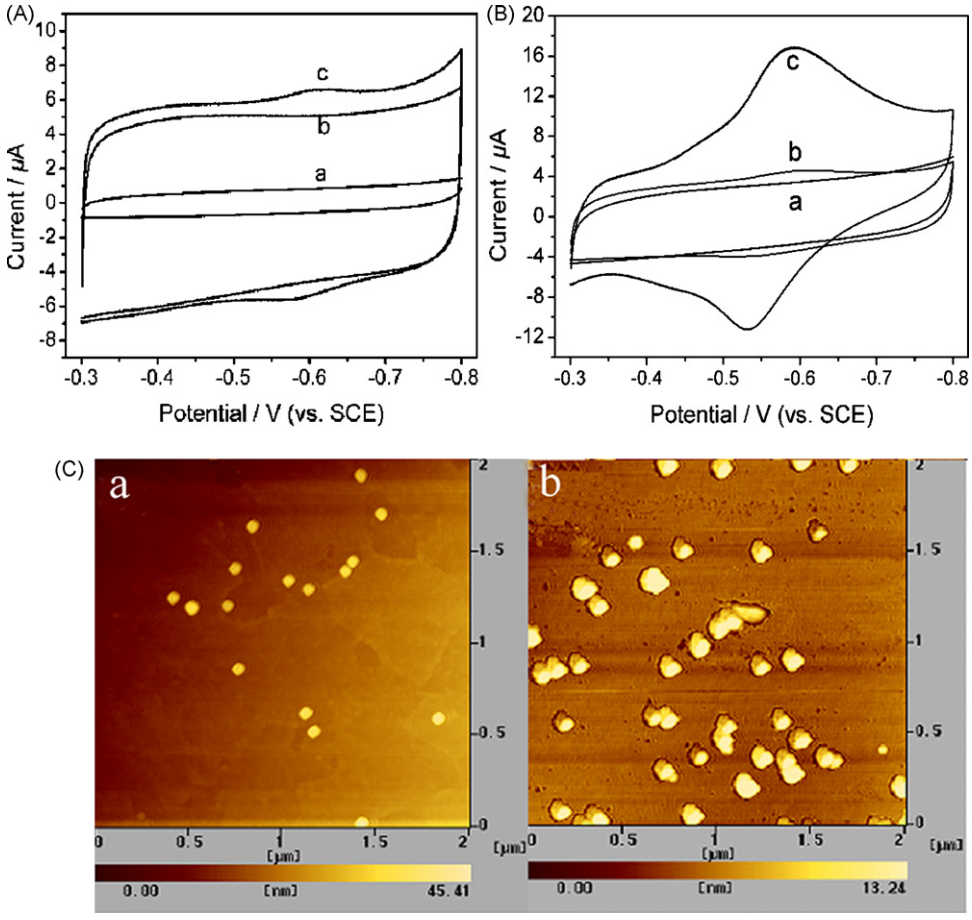

Fig. 3. (A) Cyclic voltammograms of (a) GCE, (b) GNPs/PDCNTs/GCE in 0.1 M pH 7.0 PBS, and (c) GNPs/PDCNTs/GCE in 0.1 M pH 7.0 PBS contained 2.0 mM OPD. (B) Cyclic voltammograms of HRP–Ab–Ag complexes/GNPs/PDCNTs/GCE in 0.1 M pH 7.0 PBS (a), in 0.1 M pH 7.0 PBS contained 2.0 mM OPD (b), and in 0.1M pH 7.0 PBS contained 2.0 mM OPD and 4.0 mM H_2O_2 (c). Scan rate: 100 mV s^{-1}. (C) The AFM images of GNPs (a) and HRP–GNPs–Ab_2 (b) on smooth silicon wafers.

PBS, the cyclic voltammograms of GNPs/PDCNTs/GCE and HRP–GNPs–Ab–Ag complexes covered GNPs/PDCNTs/GCE showed only weak redox peaks (curve c in Fig. 3A and curve b in Fig. 3B). When 2.0 mM OPD and 4.0 mM H_2O_2 were added to PBS, the cyclic voltammogram of HRP–GNPs–Ab–Ag complexes covered GNPs/PDCNTs/GCE showed a pair of stable and well defined redox peaks, the anodic and cathodic peak potentials were −0.532 and −0.593 V (vs. SCE), respectively (curve c in Fig. 3B), corresponding to the redox of 2,2′-diaminoazobenzene, the enzymatic product. Thus, the oxidation of OPD by H_2O_2 quickly went to completion under the catalysis of HRP. Here the HRP immobilized in the immunosensor surface retained high enzymatic catalytic activity. In addition, CNTs provided a three-dimensional homogenous matrix for the adsorption of GNPs, enhanced the immobilized amount of GNPs, facilitated more Ab_1 molecules to adsorb on the GNPs surface, and improved the stability of the immunosensor.

3.2.2. Ab_2–GNPs–HRP bioconjugates

A kind of biomaterial bearing multiple HRP labels attached to GNPs surfaces was first developed for multi-label amplification to enhance sensitivity. Our approach was to link HRP and Ab_2 to GNPs with a reaction mixture having an about 8/1 for HRP/Ab_2 molar ratio. This biomaterial was made to replace the conventional HRP–Ab_2 complex. Ab_2 and HRP were covalently linked to GNPs by a classical strategy, which could be firmly attached onto the surfaces through the interactions between GNPs and mercapto or primary amine groups of biomolecules. This process avoided protein cross-linking, which we found to form bundles of the Ab_2–GNPs–HRP bioconjugates that may deteriorate detection performance. Fig. 3C shows AFM images of isolated GNPs before and after conjugation with HRP and Ab_2. Size analysis showed that the image before conjugation had an average size of 20 nm, whereas the images of GNPs with HRP and Ab_2 attached had average sizes of 40 nm. The 20 nm increase in size for the bioconjugate GNPs was consistent with the average thickness of a monolayer of the major coating component HRP (4.0 nm × 6.7 nm × 11.7 nm, Brookhaven Protein Database) on the 20 nm GNPs surface.

The amount of antibody and HRP molecules adsorbed onto the GNPs was determined by Bradford protein assay. The Bradford protein assay is a simple procedure for determination of protein concentrations in solutions that depends upon the change in absorbance at 595 nm in Coomassie Blue G-250 upon binding of protein (Bradford, 1976). After the HRP and Ab_2 adsorption process, the HRP–GNPs–Ab_2 conjugations were precipitated by centrifugation. The sum concentrations of Ab_2 and HRP in solution before adsorption and in the supernatant after adsorption were determined by the Bradford protein assay. The difference in the amount of HRP and Ab_2 before and after adsorption was calculated and represented the amount of HRP and Ab_2 adsorbed onto the GNPs surfaces. The sum amount of Ab_2 and HRP in the stock HRP–GNPs–Ab_2 dispersion was estimated to be 14.96 μg.

To determine the ratio of active HRP in HRP–GNPs–Ab_2 conjugation, the HRP–GNPs–Ab_2 dispersion was reacted with HRP substrate OPD and H_2O_2. The reaction produced 2,2′-diaminoazobenzene with characteristic optical absorbance peak at 405 nm. This was compared to a standard curve constructed with underivatized HRP, after subtracting the background absorbance of an equivalent dispersion of underivatized GNPs. The amount of active HRP in the stock HRP–GNPs–Ab_2 dispersion was determined by these enzyme activity experiments to be 10.2 μg. From these data, the amount of Ab_2 in the HRP–GNPs–Ab_2 solution was 4.76 μg. Thus, the molar ratio of HRP and Ab_2 in the conjugations was about 8/1, which was consistent with the ratio of the initial amount.

3.2.3. Characteristic of the immunoassay

Inhibition of nonspecific binding (NSB) was critical to achieve the best sensitivity and detection limits. Thus, we developed a highly effective blocking procedure utilizing competitive binding of BSA and the detergent Tween-20, and also optimized the concentration of Ab_2–GNPs–HRP bioconjugates (1:5). Before exposure to the sample, immunosensors were incubated for 1 h with 50 μL 2% BSA + 0.05% Tween-20, then washed with 0.05% Tween-20 in buffer. For measurements, 60 μL different concentrations of Ag was incubated on the sensor surface, blocking buffer was used to wash, then the sensor was incubated with 60 μL Ab_2–GNPs–HRP bioconjugates. The washed immunosensor was then placed into an electrochemical cell containing the OPD in buffer and hydrogen peroxide. Fig. 4A shows the typical DPV detection of Ag using the Ab_2–GNPs–HRP bioconjugates based on the GNPs/PDCNTs immunosensors. In a control experiment (curve b), the immunosensor was taken through the full procedure without exposure to Ag, the peak current of 0.81 μA was little higher than the background current 0.58 μA (curve a), which might be caused by the physical adsorption of the Ab_2–GNPs–HRP bioconjugates on the GCE surface and the direct reduction of hydrogen peroxide at the GNPs/PDCNTs/GCE. However, the DPV signals were enhanced in the presence of different concentrations of Ag from 0.125 to 80 ng/mL (from curves e–n). Fig. 4B shows the plot of background-subtracted peak current versus the logarithm of the concentration of Ag. The corresponding calibration plot of response versus the logarithm of the concentration of the Ag was linear over the range from 0.125 to 80 ng/mL and was suitable for quantitative analysis. The response obtained with a protein target concentration of 0.125 ng/mL indicated a detection limit of around 40 pg/mL. Higher serum Ag levels could be detected with an appropriate dilution.

In order to prove that the Ab_2–GNPs–HRP label can improve the sensitivity of the immunosensor, we analyzed different amounts of Ag with the immunosensors by immunoreacting with the conventional HRP–Ab_2. Similar NSB blocking protocols as summarized for the Ab_2–GNPs–HRP bioconjugates were followed when using HRP–Ab_2 to measure the response of the immunosensor to Ag. Optimization of HRP–Ab_2 concentration, a major factor in minimizing NSB, was performed by evaluating the performance of dilutions of the stock HRP–Ab_2 using PBST. A 800-fold dilution gave the best detection limit. Fig. 5A shows the typical DPV detection of Ag using the HRP–Ab_2 based on the GNPs/PDCNTs immunosensor. The voltammetric peaks were well defined and the intensity was proportional to the

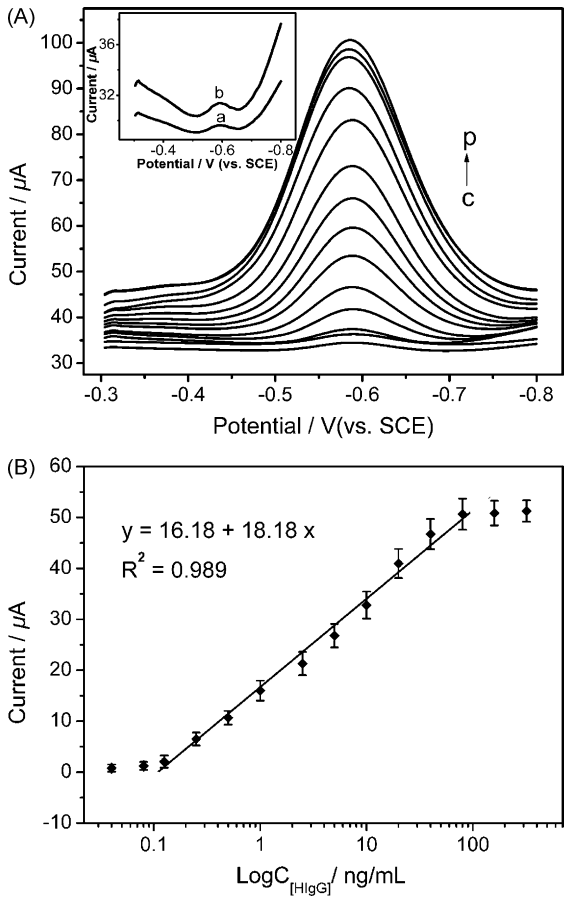

Fig. 4. (A) Typical DPV of electrochemical immunoassay using HRP–GNPs–Ab_2 conjugations in 0.1 M pH 7.0 PBS contained 2.0 mM OPD and 4.0 mM H_2O_2 with increasing HIgG concentration from (c) to (p) (0.04, 0.08, 0.125, 0.25, 0.5, 1.0, 2.5, 5.0, 10, 20, 40, 80, 160 and 320 ng/mL HIgG, respectively). Curve (a) is from the GNPs/PDCNTs modified GCE; curve (b) is from the control electrode (in the absence of HIgG). (B) The resulting calibration curve of HIgG plotted on a semi-log scale.

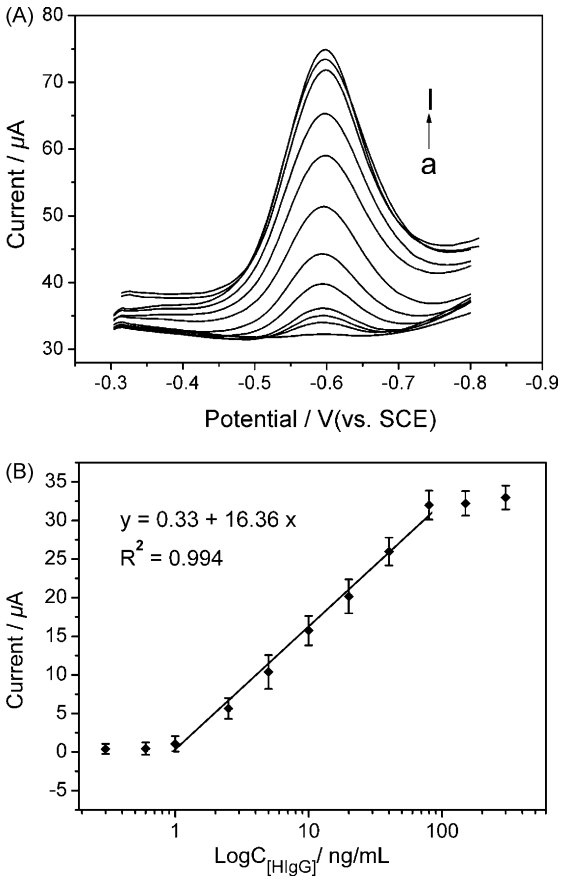

Fig. 5. (A) Typical DPV of electrochemical immunoassay using HRP–Ab_2 in 0.1 M pH 7.0 PBS contained 2.0 mM OPD and 4.0 mM H_2O_2 with increasing HIgG concentration from (a) to (l) (0, 0.25, 0.5, 1.0, 2.5, 5.0, 10, 20, 40, 80, 150 and 300 ng/mL HIgG, respectively). (B) The resulting calibration curve of HIgG plotted on a semi-log scale.

concentration of the corresponding Ag (from curves d–g). However, signal intensity was greatly decreased compared to using the Ab_2–GNPs–HRP label (cf. Fig. 4A). The corresponding calibration plot of background-subtracted peak current versus the logarithm of the concentration of Ag was linear over the range from 1.0 to 80 ng/mL and the detection limit was around 0.35 ng/mL. It can be seen that the limit of detection using HRP–Ab_2 was about nine times higher than that obtained using the HRP–GNPs–Ab_2 conjugate (40 pg/mL).

The analysis sensitivity enhance achieved using GNPs was due to a higher number of HRP molecules. However, the resulting detection limit decreased because of a lower nonspecific signal. In fact, the curve b in Fig. 4A, representing the nonspecific signal using the HRP–GNPs–Ab_2, the peak current (0.81 μA) was just a bit higher than the nonspecific signal with HRP–Ab_2 (0.68 μA, curve a in Fig. 5A). This could be explained only by the fact that, during the washing steps, the nonspecific interactions could be eliminated more easily when the antibody was attached to GNPs than when it was alone. That made the nonspecific signal at a value lower than that at which it should be considering the signal enhancement.

3.2.4. Specificity, regeneration and stability of the immunosensor

The effect of substances that might interfere with the response was studied. Using an incubation solution containing 10 ng/mL goat IgG and 10 ng/mL HIgG, the specificity of the proposed immunosensor was examined by detecting the electrochemical response. No significant difference of currents (R.S.D. = 5.1%) was observable in comparison with the result obtained in presence of only HIgG. The increase of goat IgG concentration to some extent did not lead to a significant signal change. The regeneration of the proposed immunosensor was tested by washing the immunosensor with a stripping buffer of 0.1 M pH 3.5 glycine–HCl solution for the purpose of removing HIgG and Ab_2 from Ab_1 after each determination. In the experiment, it had repeated five times consecutive measurements and a R.S.D. of 6.5% was acquired. When the Ab_1/GNPs/CNTs modified immunosensor was stored in the refrigerator at 4 °C, no obvious change was found in the response over 30 days. The sensor depicted a quite satisfying stability, which retained more than 95% of its initial response. Good stability can be attributed to the strong interactions between the GNPs/CNTs and Ab_1.

Table 1
Comparison of serum HIgG levels determined using two methods

Serum samples	1	2	3	4	5
Immunosensor (ng/mL)[a]	0.27	9.58	22.6	67.5	75.6
ELISA[a]	0.25	9.12	21.2	65.1	72.5
Relative deviation (%)	8.0	5.1	6.6	3.7	4.3

[a] The average value of five successive determinations.

3.2.5. Application of the immunosensor in human serum

The feasibility of the immunoassay system for clinical applications was investigated by analyzing several real samples, in comparison with the ELISA method. These serum samples were diluted to different concentrations with a PBS of pH 7.0.

Table 1 describes the correlation between the partial results obtained by the proposed immunosensor and ELISA method. It obviously indicates that there is no significant difference between the results given by two methods, that is, the developed versatile immunoassay may provide an interesting alternative tool for detection protein in clinical laboratory.

4. Conclusion

It has been demonstrated here, for the first time, that GNPs/CNTs nanohybrids were used to construct an electrochemical immunosensor for highly sensitive immunoassay. In our procedure, a novel label system consisting of HRP molecules and antibody conjugated to GNPs at high HRP/Ab_2 ratio was used to detect human IgG as a model protein. The developed label method was versatile, offers enhanced performances, and could be easily extended to other protein detection schemes as well as in DNA analysis.

Acknowledgments

We greatly appreciate the support of the National Natural Science Foundation of China (Grant Nos. 20325516, 20635020, 20521503, 20575026). This work is also supported by National Basic Research Program of China (2006CB933201). The authors thank Prof. Jinan Zhang and Dr. Di Yang from Research Institute of Cardiovascular Disease of First Affiliated Hospital of Nanjing Medical University for their invaluable advice throughout the project.

References

Ambrosi, A., Castaneda, M.T., Killard, A.J., Smyth, M.R., Alegret, S., Merkoci, A., 2007. Anal. Chem. 79, 5232–5240.
Bard, A.J., Faulkner, L.R., 1980. Wiley, New York.
Bradford, M.M., 1976. Anal. Biochem. 72, 248–254.
Cui, R.J., Pan, H.-C., Zhu, J.-J., Chen, H.-Y., 2007. Anal. Chem. 79, 8494–8501.
Daniel, M.C., Astruc, D., 2004. Chem. Rev. 104, 293–346.
Das, J., Aziz, M.A., Yang, H., 2006. J. Am. Chem. Soc. 128, 16022–16023.
Enustun, B.V., Turkevich, J., 1963. J. Am. Chem. Soc. 85, 3317–3328.
Hansen, J.A., Mukhopadhyay, R., Hansen, J., Gothelf, K.V., 2006. J. Am. Chem. Soc. 128, 3860–3861.
Hayat, M.A. (Ed.), 1989. Academic Press, New York.
Jiang, K., Eitan, A., Schadler, L.S., Ajayan, P.M., Siegel, R.W., 2002. Nano Lett. 3, 275–277.
Katz, E., Willner, I., 2004. Angw. Chem. Int. Ed. 43, 6042–6108.
Katz, E., Willner, I., Wang, J., 2004. Electroanalysis 16, 19–44.
Liu, J., Rinzler, A.G., Dai, H., Hafuer, J.H., Bradley, R.K., Boul, P.J., Lu, A., Iverson, T., Shelimov, K., Huffman, C.B., Rodriguez-mcscias, F., Shon, Y.-S., Lee, T.R., Colbert, D.T., Smalley, R.E., 1998. Science 280, 1253–1256.
Mamedov, A.A., Kotov, N.A., Prato, M., Guldi, D.M., Wicksted, J.P., Hirsch, A., 2002. Nat. Mater. 1, 190–194.
Merkocüi, A., Aldavert, M., Marin, S., Alegret, S., 2005. Trends Anal. Chem. 24, 341–349.
Munge, B., Liu, G., Collins, G., Wang, J., 2005. Anal. Chem. 77, 4662–4666.
Pumera, M., Aldavert, M., Mills, C., Merkocüi, A., Alegret, S., 2005. Electrochim. Acta 50, 3702–3707.
Porstmann, B., Porstmann, T., 1988. In: Ngo, T.T (Ed.), Plenum Press, New York, pp. 57–84.
Rouse, J.H., Lillehei, P.T., 2003. Nano Lett. 3, 59–62.
Schneider, B.H., Dickinson, E.L., Vach, M.D., Hoijer, J.V., Howard, L.V., 2000a. Biosens. Bioelectron. 15, 13–22.
Schneider, B.H., Dickinson, E.L., Vach, M.D., Hoijer, J.V., Howard, L.V., 2000b. Biosens. Bioelectron. 15, 597–604.
Wang, J., 2005. Small 1, 1036–1043.
Wang, J., Liu, G., Rasul, M., 2003. J. Am. Chem. Soc. 126, 3010–3011.
Wang, L., Guo, S., Huang, L., Dong, S., 2007. Electrochem. Commun. 9, 827–832.
Wu, B.Y., Houb, S.H., Yin, F., Zhao, Z.X., Wang, Y.Y., Wang, X.S., Chen, Q., 2007. Biosens. Bioelectron. 22, 2854–2860.
Xu, Y.W. (Ed.), 1997. Science Press, Beijing.
Yu, X., Munge, B., Patel, V., Jensen, G., Bhirde, A., Gong, J.D., Kim, S.N., Gillespie, J., Gutkind, J.S., Papadimitrakopoulos, F., Rusling, J.F., 2006. J. Am. Chem. Soc. 128, 11199–11205.
Zhang, C., Zhang, Z., Yu, B., Shi, J., Zhang, X., 2002. Anal. Chem. 74, 96–99.
Zhao, J., Henkens, R.W., Stonehuerner, J., O′Daly, J.P., Crumbliss, A.L., 1992. J. Electroanal. Chem. 327, 109–119.